Elastic behaviour of pure cobalt near the spin-reorientation phase transition

1991 J. Phys.: Condens. Matter 3 2263

(http://iopscience.iop.org/0953-8984/3/14/005)

J. Phys.: Condens. Matter 3 (1991) 2263–2272. Printed in the UK

Elastic behaviour of pure cobalt near the spin-reorientation phase transition

J-E Bidaux† and B Cao
Institut de Génie Atomique, Ecole Polytechnique Fédérale de Lausanne, CH-1015 Lausanne, Switzerland

Received 9 July 1990, in final form 17 December 1990

Abstract. The elastic behaviour of pure cobalt is investigated in the vicinity of the spin-reorientation phase transition. Near each of the two transition temperatures $T_l \simeq 535$ K and $T_u \simeq 595$ K, a step-like change of the elastic constant c_{33} and a softening of c_{44} are observed. In a magnetic field applied parallel to the hexagonal axis, the lower transition (at T_l) is shifted to higher temperatures while the upper transition (at T_u) is suppressed. All these observations are in good agreement with calculations based on a thermodynamic theory.

1. Introduction

Pure cobalt undergoes a spontaneous reorientation of the magnetization in the temperature range 530–600 K [1]. At $T_l \simeq 535$ K, the first anisotropy constant K_1 becomes zero [2] and the spins rotate from a direction parallel to the hexagonal axis (c axis) towards the basal plane. Because the second anisotropy constant K_2 remains positive [3], the reorientation proceeds continuously. Finally, the spins reach the basal plane at $T_u \simeq 595$ K. It can be shown that the two temperatures T_l and T_u are each associated with a second-order Landau-type transition [3]. Between T_l and T_u, owing to the weak basal plane anisotropy [4], the spins describe a conical structure.

Taborov and Tarasov [5] first observed ultrasonic effects related to this transition. A single attenuation peak was found near 550 K, which was interpreted as a manifestation of resonant interaction between elastic and spin waves resulting from a lowering of the spin-wave frequency due to the vanishing of the anisotropy.

This effect was studied in more detail by Wallace [6], who observed a decrease in elastic constants and an increase in attenuation in the same temperature range. The anomalies were apparently removed by a saturating magnetic field applied along the c axis, suggesting domain-wall effects. However, as pointed out by Wallace, a more detailed description of the phenomenon would require further investigation over a wider temperature range. (Their measurements were limited to $T < 570$ K.)

In the present study, measurements of elastic moduli were extended up to 700 K and also for various values of the applied magnetic field. This allowed us to show that the elastic moduli anomalies are mainly bulk effects, though domains can be involved to some extent. Accordingly, the main features of elastic moduli and their magnetic field dependence can be explained by thermodynamic arguments. Here, we use the theory of Gorodetsky and Lüthi [7–9], originally developed to account for elastic anomalies

† Present address: Centro Atomico Bariloche, 8400 SC de Bariloche (RN), Argentina.

Table 1.

Anisotropy constants[a]	$K_1(T) = 8.56 \times 10^5 - 1.6 \times 10^3 T$ (J m^{-3}) $K_2(T) = 2.25 \times 10^5 - 3 \times 10^2 T$ (J m^{-3}) (where T is in kelvins)
Magnetostriction coefficients[b]	$\lambda_A = -6.88 \times 10^{-5} + 8.0 \times 10^{-8} T$ $\lambda_B = -1.33 \times 10^{-4} + 9.6 \times 10^{-8} T$ $\lambda_C = 1.53 \times 10^{-4} - 7.2 \times 10^{-8} T$ $\lambda_D = -1.54 \times 10^{-4} + 1.52 \times 10^{-7} T$
Elastic constants[c]	$c^0_{33} = 382.2 - 0.086T$ (GPa) $c^0_{13} = 104.7 - 0.0078T$ (GPa) $c^0_{44} = 85.5 - 0.034T$ (GPa)
Saturation magnetization ($T \simeq 550$ K)[d]	$4\pi M = 17 \times 10^3$ G

[a] *Landolt–Börnstein* 1986 New Series III/19a (Berlin: Springer) p 44
[b] *Landolt–Börnstein* 1986 New Series III/19a (Berlin: Springer) p 50
[c] *Landolt–Börnstein* 1986 New Series III/11 (Berlin: Springer) p 174
[d] *Landolt–Börnstein* 1962 6 Aufl Bd II/9 (Berlin: Springer) p 1–17

related to spin reorientation in tetragonal antiferromagnetic orthoferrites, and apply it to the case of hexagonal ferromagnetic cobalt.

2. Theory

The total free-energy density necessary to describe elastic behaviour associated with spin reorientation during the phase transition in cobalt is

$$F = F_a + F_{me} + F_{el} + F_h \tag{1}$$

where F_a is the magnetocrystalline anisotropy energy, F_{me} the magnetoelastic energy, F_{el} the elastic energy and F_h the interaction energy with an external magnetic field.

In the absence of an applied magnetic field, the orientation of magnetization of a ferromagnetic crystal is controlled by the anisotropy energy, which for hexagonal cobalt [10] is given by

$$F_a = K_1(T)\sin^2\theta + K_2(T)\sin^4\theta \tag{2}$$

where $K_1(T)$ and $K_2(T)$ are the first and second magnetocrystalline anisotropy constants, respectively, and θ the angle between the c axis and the internal magnetization $\boldsymbol{M}$. In the above equation we have neglected higher-order terms in θ as well as the dependence on azimuthal angle φ, which have been found to be negligible in cobalt [4, 10]. The temperature dependence of the orientation of the ferromagnetic moment $\boldsymbol{M}$ can be obtained by using the equilibrium and stability conditions $\partial F_a/\partial\theta = 0$ and $\partial^2 F_a/\partial\theta^2 > 0$. Thus

$$\begin{array}{lll} \theta = 0 & K_1 > 0 & T \leqslant T_l \\ \sin^2\theta = -K_1/2K_2 & 0 > K_1 > -2K_2 & T_l < T < T_u \\ \theta = \pi/2 & K_1 < -2K_2 & T \geqslant T_u. \end{array} \tag{3}$$

Given the temperature dependence of K_1 and K_2 (see table 1), one can calculate the angle θ as a function of temperature. One obtains (figure 1) a magnetization that is parallel to the c axis for $T \leqslant T_l$ ($T_l \simeq 535$ K), then reorients itself continuously towards the basal plane ($T_l < T < T_u$), which is reached at $T = T_u$ ($T_u \simeq 595$ K).

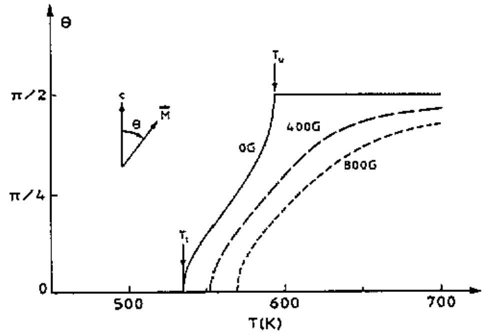

Figure 1. Calculated temperature dependence of the angle θ between magnetization and the c hexagonal axis at various magnetic fields applied along the c axis. T_l = lower transition temperature, T_u = upper transition temperature.

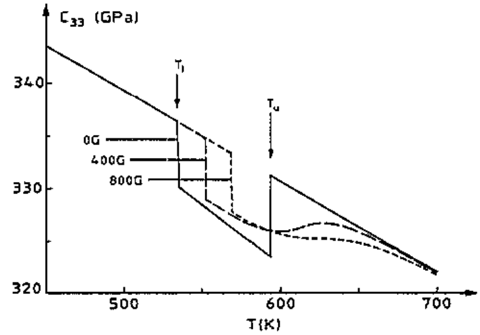

Figure 2. Calculated temperature dependence of elastic constant c_{33} at various magnetic fields applied along the c axis.

Therefore, we have two displacive second-order phase transitions, one at T_l with order parameter θ and the other at T_u with order parameter $\pi/2 - \theta$. Since the second derivative $\partial^2 F_a/\partial\theta^2$ of the free energy with respect to order parameter vanishes at T_l and T_u, the spin system becomes unstable and the two transitions are associated with a soft mode [3, 7].

2.1. *Effect of an applied magnetic field*

Neglecting the contribution of the demagnetizing field, which is very small for the geometry used in the present experiments, the interaction energy of the magnetization M with an external magnetic field H applied along c axis can be written as

$$F_h = -HM\cos\theta. \tag{4}$$

The minimization of $F_a + F_h$ yields the following solutions for the temperature dependence of the order parameter θ:

$$\begin{aligned} &\theta = 0 && K_1 > -\tfrac{1}{4}HM \quad T < T_l \\ &(K_1+K_2)\sin(2\theta) - \tfrac{1}{2}K_2\sin(4\theta) + HM\sin\theta = 0 && K_1 < -\tfrac{1}{4}HM \quad T > T_l \end{aligned} \tag{5}$$

which is represented in figure 1 for various values of the applied magnetic field. It appears that the field stabilizes the low-temperature phase, shifting the lower transition temperature T_l to higher temperatures. Using equation (5) we find that the magnitude of the shift is

$$\mathrm{d}T_l/\mathrm{d}H = -(\mathrm{d}K_1/\mathrm{d}T)^{-1}(M/2). \tag{6}$$

Assuming a reasonably linear temperature dependence of K_1 in the domain of interest, equation (6) predicts a displacement of T_l proportional to the intensity of the applied magnetic field.

In addition, another important effect of the magnetic field is to impede the complete rotation of the magnetization towards the basal plane: the upper transition is suppressed.

2.2. *Elastic behaviour*

The magnetoelastic interaction energy F_{me} for hexagonal symmetry has been given in the literature [12]. In the special case of propagation along the c axis, the expression reduces in Voigt notation to

$$F_{me} = (B_{33} - B_{13})\varepsilon_{zz}\cos^2\theta + B_{44}(\varepsilon_{xz}\cos\varphi + \varepsilon_{yz}\sin\varphi)\sin(2\theta) \tag{7}$$

where the B_{ij} are the components of the magnetoelastic tensor, ε_{ij} the components of the strain tensor and φ the azimuthal angle of the magnetization.

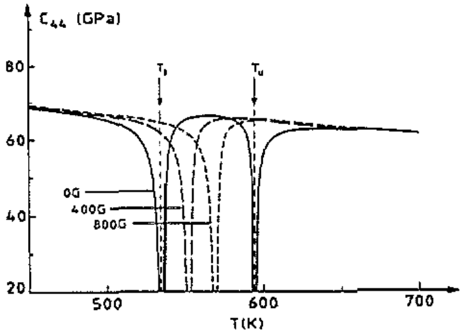

Figure 3. Calculated temperature dependence of elastic constant c_{44} at various magnetic fields applied along the c axis.

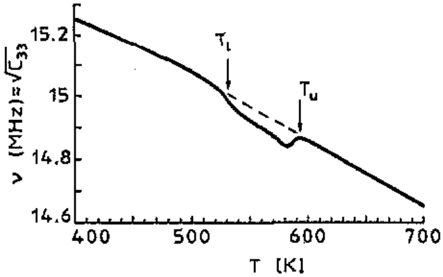

Figure 4. Standing-wave frequency ν of the longitudinal mode (c_{33}) parallel to the c axis measured as a function of temperature.

Also the elastic energy is

$$F_{el} = \tfrac{1}{2}c_{33}^0\varepsilon_{zz}^2 + \tfrac{1}{2}c_{44}^0(\varepsilon_{xz}^2 + \varepsilon_{yz}^2). \tag{8}$$

The anomalies of elastic constants related to the motion of the order parameter θ can be calculated using the formula [13]

$$c_{ij} = c_{ij}^0 - \left[\frac{\partial}{\partial\varepsilon_{ij}}\left(\frac{\partial F}{\partial\theta}\right)_{\varepsilon_{ij}}\right]_\theta^2 \left(\frac{\partial^2 F}{\partial\theta^2}\right)_{\varepsilon_{ij}}^{-1} \tag{9}$$

where F is the total free-energy density given in equation (1) and c_{ij}^0 the 'normal' linear elastic constants in the absence of a phase transition.

Here we do not take into account the effect of the strain-induced azimuthal rotation of the magnetization, which could, as we shall see later, also give a contribution to the elastic shear constant c_{44}.

For longitudinal waves one obtains

$$c_{33} = c_{33}^0 - \tfrac{1}{2}\frac{(B_{33} - B_{13})^2\sin(2\theta)}{(K_1 + K_2)\cos(2\theta) - K_2\cos(4\theta) + \frac{1}{2}HM\cos\theta} \tag{10}$$

and for shear waves

$$c_{44} = c_{44}^0 - \frac{2B_{44}^2\cos(2\theta)\sin^2\varphi}{(K_1 + K_2)\cos(2\theta) - K_2\cos(4\theta) + \frac{1}{2}HM\cos\theta} \tag{11}$$

where $\theta = \theta(T)$ is the equilibrium value given by equation (5). In the above formula $\sin^2\varphi$ can be replaced by its average value $\langle\sin^2\varphi\rangle = \frac{1}{2}$ over all the possible domains, each domain being specified by a given angle φ on the cone of the easy axis of magnetization. For a quantitative evaluation of the elastic constants, the magnetoelastic coupling constants B_{ij} are needed. These are related to the magnetostriction coefficients λ_i. By a method similar to that used by Kittel for cubic symmetry [14, 30], we obtain

$$\begin{aligned}(B_{33} - B_{13}) &= c_{13}^0(\lambda_A + \lambda_B) + c_{33}^0\lambda_C \\ B_{44} &= \tfrac{1}{2}c_{44}^0(\lambda_A + \lambda_C - 4\lambda_D).\end{aligned} \tag{12}$$

Using available data of magnetostriction coefficients and elastic constants c_{ij}^0 (see table 1), the elastic constants c_{33} and c_{44} have been calculated and are plotted on figures 2 and 3. The predicted behaviour of the elastic constants is the following.

(i) *At zero field.* The elastic constant c_{33} exhibits a step-like discontinuity at both temperatures T_l and T_u. Between T_l and T_u, c_{33} is a monotonically decreasing function of temperature. These features are in close relation with the existence of a quadratic coupling between ε_{zz} and order parameter θ (equation (7)). In contrast, because of the linear coupling between ε_{yz} or ε_{xz} and θ, c_{44} reflects the existence of a magnetic instability (θ instability) and shows a softening at both T_l and T_u.

(ii) *In an applied magnetic field.* The temperature T_l is shifted but the elastic behaviour near T_l is not modified. On the contrary, the disappearance of the upper transition at T_u leads to a profound modification of the elastic constants. The step-like discontinuity in c_{33} observed at zero field is smoothed out. In addition, the softening of c_{44} is completely removed.

3. Experimental details

The temperature dependence of c_{33} was measured by using a continuous-wave ultrasonic resonator [15] working in the transmission mode. For a description of the apparatus see [16–18]. Basically, the technique consisted of measuring one of the standing-wave frequencies ν_n allowed in a composite resonator made of the sample and two piezoelectric transducers. For transducers of negligible mass and in the special case of the longitudinal mode parallel to the c axis we have

$$\nu_n = n(v_L/2l) \tag{13}$$

where v_L is the phase velocity of the wave, n the index of the harmonic considered (here typically $n = 20$, $\nu \simeq 20$ MHz) and l the sample length; v_L is connected to the elastic constant c_{33} by

$$c_{33} = \rho v_L^2 \tag{14}$$

where ρ is the mass density of the sample. Because the transition is second order, the variations in length (here of the order of the magnetostriction coefficient $\lambda_C \simeq 10^{-4}$) as well as in density during the spin reorientation are very small and can be neglected. Therefore we have

$$c_{33} \sim \nu_n^2 \tag{15}$$

and the temperature variations of the elastic constant could be directly followed by measuring the frequency of the appropriate mode. The sample used was a cylindrical single crystal of 99.98% cobalt with 10 mm diameter and 6 mm length provided by Johnson Matthey. The sample was spark cut and polished with parallel faces oriented normal to the c hexagonal axis. The parallelism was better than 10^{-2} deg. Bonding was achieved using the coupling cement ZGM Krautkrämer, which provided good adhesion in this temperature range. The measurements were made at a constant heating rate of 1 K min^{-1}. The temperature was measured by a platinum resistor mounted close to the sample and controlled by a PID system [16] within 0.1 K.

Because of technical problems related to bonding and high attenuation, c_{44} was not measured with this same equipment but by means of a low-frequency ($\nu \sim 1$ Hz) inverted torsional pendulum. For a description of the instrument see [19]. The frequency of the fundamental torsional mode of the system sample–inertia arm is related to the shear modulus G of the sample by [20]

$$\nu = \alpha G^{1/2} \tag{16}$$

where α is a factor depending on the geometry and mass of the whole system, which is, in our case, not temperature-dependent. Starting with a cobalt single crystal of 99.998% purity provided by Goodfellows Co., a sample was spark cut in the shape of a wire of length 10 mm and section $0.4 \times 0.4\ \mathrm{mm}^2$. This sample shape [21] as well as the classical cylindrical shape allows the excitation of a pure shear mode of the type ε_{yz} and ε_{xz} ($z \| c$ axis). By orienting the crystal so that the c axis is along the wire axis, we have $G = c_{44}$ [22] and accordingly the elastic constant c_{44} could be measured using (16).

The elastic constants calculated in section 2 are the isothermal elastic constants. For ultrasonic measurements, isothermal conditions are generally not fulfilled and are more likely under adiabatic conditions. Therefore, for quantitative evaluation of Δc_{33}, a correction factor should be included [13]. However, it is possible to show that this contribution is small for the present case and thus will be neglected.

4. Results

4.1. Elastic constant c_{33}

Figure 4 gives the temperature dependence of the elastic constant c_{33} through the temperature dependence of the frequency of the longitudinal mode parallel to the c axis (we have $c_{33} = \nu^2$, $\Delta c_{33}/c_{33} = 2\Delta\nu/\nu$). We observe experimentally that the behaviour of c_{33} is in good qualitative agreement with the theoretical predictions of figure 2. A step-like decrease in frequency is observed at T_l followed by a step-like increase at T_u. The magnitude of the effect is theoretically $(\Delta c_{33}/c_{33})_{th} \simeq 2\%$. Actually we observe experimentally only $(\Delta c_{33}/c_{33})_{exp} \simeq 0.8\%$. This discrepancy could arise from the uncertainty in the available value of the anisotropy coefficient K_2 and can be as high as 100% because anisotropy coefficients depend strongly on the microstructure [2], which can vary from sample to sample [11]. But it could also indicate that the frequency is too high for the spin system to achieve complete magnetic equilibrium under the rapidly varying strain field as was assumed in our static calculations. A possible retarding mechanism is a relaxation due to eddy currents [23].

The increase of the elastic constants at T_u is more pronounced than the decrease at T_l. This agrees with the calculation and is due to the temperature decrease of K_2. At zero field equation (9) can actually be written more simply as

$$c_{33} = c_{33}^0 - (B_{33} - B_{13})^2/2K_2. \tag{17}$$

Accordingly, it is clear that a decrease in K_2 (see table 1) corresponds to an enhanced c_{33} anomaly.

Domain-wall motion should not contribute to c_{33} [24] because the ε_{zz} term in the magnetoelastic energy (equation (7)) does not depend on the domain considered (each domain is specified by the angle φ on the cone of the easy axis of magnetization). In other words ε_{zz} cannot favour one domain with respect to another. Note that at T_l we have $K_1 = 0$ and therefore the domain walls vanish [25].

4.2. Elastic constant c_{44}

Figure 5 shows the shear mode at zero field. The frequency ν shifts to two well defined minima, which can be interpreted as due to the softening of c_{44} at T_l and T_u in agreement with figure 3. Actually, the softening is not so pronounced as the predicted one. This might be explained by inhomogeneities in the material. The martensitic FCC → HCP phase transition, which occurs at about 400 °C, produces a very high density of crystal

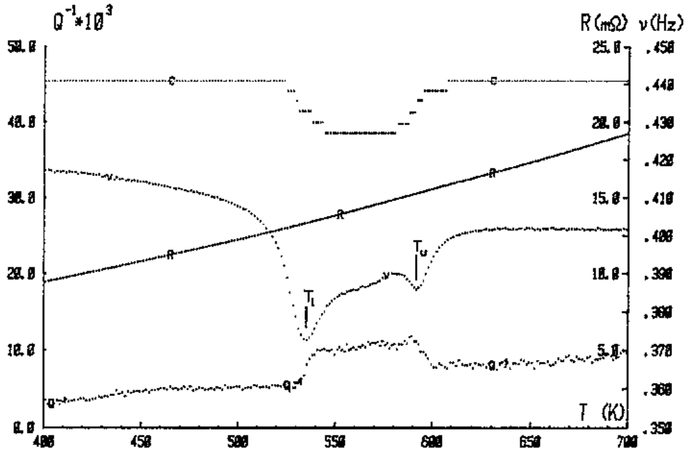

Figure 5. Frequency ν and damping Q^{-1} of the torsional mode (c_{44}) of a wire whose axis lies parallel to the c hexagonal axis measured as a function of temperature. Also measured are electrical resistivity R and spontaneous torsion C (arbitrary scale).

defects, especially stacking faults [26]. On the other hand, smoothing of the effect could also come from the rather high finite strain amplitude ($\varepsilon \sim 10^{-6}$) used in c_{44} measurements, allowing anharmonicity to contribute in contrast to the hypothesis in our calculations.

Between T_l and T_u, we observe that the damping Q^{-1} increases. At such a low frequency (of the order of hertz) magnetic damping is most likely of magnetomechanical hysteresis type related to domain-wall motion [23]. This interpretation is consistent with the fact that, between T_l and T_u, ε_{yz} and ε_{xz} terms in the magnetoelastic energy (equation (7)) depend on the angle φ because $\sin(2\theta) \neq 0$. Therefore, during spin orientation, certain domains are favoured by strain, and domain-wall motion occurs. At this point, one might raise the following question: Can domain-wall motion explain the c_{44} anomaly as well? If this were the case the relative magnitude of the c_{44} anomaly should be of the same order as that of the damping [23], that is

$$(\Delta c_{44}/c_{44})_{\mathrm{dw}} \sim Q^{-1} \simeq 5 \times 10^{-3}.$$

In fact, this value is much lower than the observed decrease of c_{44} (figure 5). Therefore, if domain-wall motion can explain damping, it cannot account for elastic constant anomalies, which are more likely bulk effects.

In figure 5 is shown the electrical resistivity and the spontaneous torsion C of the specimen measured in the same experiment together with frequency and damping. Resistivity does not show any anomaly whereas the torsion C exhibits a characteristic behaviour. Since a precise quantitative measurement of this torsional strain was not made, we will only try to interpret it qualitatively. As for elastic constants we will use thermodynamic arguments. The equilibrium torsional strain ε_{xz}, which minimizes the total energy, is written as [14]

$$\varepsilon_{xz} = -\tfrac{1}{2}(\lambda_{\mathrm{A}} + \lambda_{\mathrm{C}} - 4\lambda_{\mathrm{D}}) \sin(2\theta) \cos\varphi \qquad (18)$$

where λ_{A}, λ_{C} and λ_{D} are the magnetostriction coefficients and θ is the equilibrium value, which is a function of temperature given in equation (3). Because $\sin(2\theta)$ is different from zero between T_l and T_u, magnetostriction will occur, which reaches its maximum

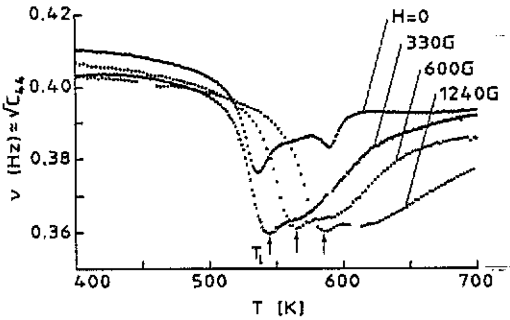

Figure 6. Temperature dependence of the frequency of the torsional mode (c_{44}) at various magnetic fields applied along the c axis. The shift of the temperature T_l associated with the lower transition temperature is indicated by the arrows.

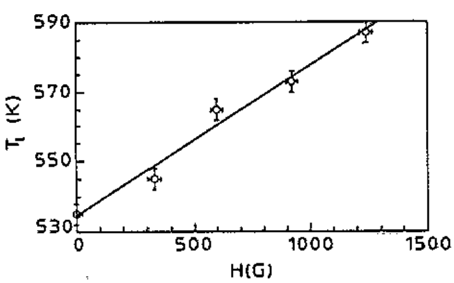

Figure 7. Shift of the temperature T_l associated with the lower transition temperature as a function of applied magnetic field along the c axis.

value $\frac{1}{2}(\lambda_A + \lambda_C - 4\lambda_D) \simeq 10^{-4}$ at $\theta = 45°$ and returns to zero after spin reorientation is completed. This is what we observe in figure 5. This is an interesting case of magnetostriction produced not by an external magnetic field but by a spontaneous rotation of internal magnetization. The predicted magnitude of the effect is of the order of 10^{-4}, which is easy to observe with a torsional pendulum. Note finally that the observation of a net magnetostriction requires that the mean value of $\cos\varphi$ over the different domains is not zero, which seems to be possible only in a macroscopically magnetized sample.

4.3. *Effect of applied magnetic field*

Figure 6 shows the effect of a magnetic field applied along the c axis. In agreement with the calculations of figure 3, the main effect of the applied field is to shift the frequency dip corresponding to the lower transition to higher temperatures. As shown in figure 7, the temperature displacement is a linear function of the applied field. By mean-square analysis of experimental data we deduce that

$$(\mathrm{d}T_l/\mathrm{d}H)_{\mathrm{exp}} \simeq 42\ \mathrm{K\ kG^{-1}}$$

which is in excellent agreement with the theoretical value

$$(\mathrm{d}T_l/\mathrm{d}H)_{\mathrm{th}} = -(\mathrm{d}K_1/\mathrm{d}T)^{-1}(M/2) \simeq 42.3\ \mathrm{K\ kG^{-1}}$$

where the data of table 1 are used for evaluation.

In addition, we observe in figure 6 that the frequency dip occurring at the upper transition at zero field does not appear any more under an applied field as predicted by the theory. However, a frequency anomaly remains for $T > T_l$ until the complete spin reorientation is achieved. This effect, which is not predicted in our calculations, could be due to the fact that, as mentioned in section 2, we have only taken into account changes in elastic constants related to the motion of order parameter θ. However, in the case of c_{44}, azimuthal motion (in φ) can also be induced. But this contribution cannot be taken into account without introducing higher-order φ-dependent terms in the anisotropy energy, the amplitude of which is still not well known [4] especially at high temperatures. Another explanation could be the effect of domain walls. This effect is certainly zero for $T < T_l$ but not during spin reorientation. In fact, according to the expression for magnetoelastic energy (equation (7)), this contribution should be maximum for $\theta = 45°$, which could explain also the slight minimum observed on the high-temperature side of the softening (figure 6).

5. Discussion

Our results are fully consistent with the previous results of Wallace [6]. It is now clear that the anomalies in elastic properties do not disappear under an applied magnetic field but are simply shifted to higher temperatures. In the case of Wallace, who used a magnetic field of 10 kG, it means that the transition is pushed inside the FCC phase. It does not, however, imply that the anomalies are domain-wall effects. On the contrary, we have shown that the main features of the results can be explained by simple thermodynamic arguments. In this sense, our interpretation of the observed anomalies is similar to that of Taborov and Tarasov [5].

Although it is apparently the first time that the two softening modes of elastic constants have been observed in cobalt, similar effects have already been observed in rare-earth orthoferrites and other compounds by Gorodetsky and coworkers [9]. Similar behaviour could also be expected for gadolinium, which has a ferromagnetic ordering at low temperature and also exhibit a spin-reorientation phase transition. Actually, in this case, the double softening is not observed [27] owing to incomplete spin reorientation. In addition, the effect of the magnetic field is more complex and different interpretations have been proposed [28, 29].

Finally, one could question the neglect of fluctuations. As shown in detail by Levinson *et al* [3], owing to the long-range interactions involved in this displacive-type transition, fluctuations would play a significant role only in a very narrow temperature range $(T - T_c)/T_c \sim 10^{-8}$ near the transition temperature (where T_c can be either T_l or T_u). It is clear that in our experiments it was not possible to observe such effects.

Acknowledgments

This work was partially supported by the Swiss National Science Foundation. The authors are grateful to Professor M Ahlers, Dr S Sathish and Professor W Benoit for critical reading of the manuscript.

References

[1] Bertaut E F, Delapalme A and Pauthenet R 1963 *Solid State Commun.* 1 81
[2] Ono F and Yamada O 1979 *J. Phys. Soc. Japan* **46** 462
[3] Levinson L, Luban M and Shtrikman S 1969 *Phys. Rev.* **187** 715
[4] Bozorth R M 1954 *Phys. Rev.* **96** 311
[5] Taborov V F and Tarasov V F 1967 *IEEE Trans. Son. Ultrason.* **SU-14** 1

[6] Wallace W 1973 *Proc. ICIFUAS* ed D Lenz and K Lücke (Berlin: Springer) p 161
[7] Gorodetsky G and Lüthi B 1970 *Phys. Rev.* B **2** 3688
[8] Gorodetsky G and Shtrikman S 1980 *J. Appl. Phys.* **51** 1127
[9] Gorodetsky G, Hornreich R M, Shaft S, Sharon B, Shaulov A and Wanklyn B M 1977 *Phys. Rev.* B **16** 515
[10] Ono F 1981 *J. Phys. Soc. Japan* **50** 2564
[11] Paige D M, Szpmar B and Tanner B K 1984 *J. Magn. Magn. Mater.* **44** 239
[12] Dobrov W 1964 *Phys. Rev.* **134** A734
[13] Rehwald W 1973 *Adv. Phys.* **22** 721
[14] Kittel C 1949 *Rev. Mod. Phys.* **21** 541
[15] Bolef D I and Miller J G 1971 *Physical Acoustics* vol VIII, ed W P Mason and R N Thurston (New York: Academic) p 96
[16] Kulik A and Bidaux J E 1987 *J. Physique Coll.* **48** C8 335
[17] Bidaux J E 1988 *PhD Thesis* EPFL, Lausanne
[18] Kulik A, Bidaux J E, Gremaud G and Sathish S 1988 *Ultrasonic Signal Processing* ed A A Lippi (Singapore: World Scientific) p 355
[19] Baur J and Kulik A 1983 *J. Physique Coll.* **44** C9 357
[20] Nowick A S and Berry B S 1972 *Anelastic Relaxation in Crystalline Solids* (New York: Academic Press) p 626
[21] Timoshenko S and Goodier J N 1951 *Theory of Elasticity* (New York: McGraw-Hill) p 260
[22] Novick and Berry p 145 in [20]
[23] Novick and Berry p 524 in [20]
[24] Fisher E S and Dever D 1967 *Trans. Met. Soc. AIME* **239** 48
[25] Chikazumi S 1964 *Physics of Magnetism* (New York: Wiley) p 186
[26] Hitzenberger C, Karnthaler H P and Korner A 1985 *Acta Metall.* **33** 1293
[27] Klimker H and Rosen M 1973 *Phys. Rev.* B **7** 2054
[28] Freyne F 1972 *Phys. Rev.* B **5** 1327
[29] Levinson L M and Shtrikman S 1971 *J. Phys. Chem. Solids* **32** 981
[30] Birss R R 1964 *Symmetry and Magnetism* vol III (Amsterdam: North-Holland) p 197